III-Nitrides for sensing at high temperatures

Goutam Koley
Department of Electrical and Computer Engineering
Clemson University, USA
Email: gkoley@clemson.edu

Makhluk Hossain Prio
Department of Electrical and Computer Engineering
Clemson University, USA
Email: mprio@g.clemson.edu

Ferhat Bayram
Coherent Corporation
Dallas, Texas, USA
Email: fbayram@g.clemson.edu

Durga Gajula
The Institute for Electronics and Nanotechnology (IEN), USA
Georgia Institute of Technology
Email: dgajula3@gatech.edu

Abstract— **There is a significant need for high temperature pressure sensors for applications in aerospace, automotive, chemical processing, nuclear power and petroleum industries. While Si based piezoresistive pressure sensors are one of the most prevalent pressure sensors, due to degradation in their electrical properties related to the generation of thermal carriers and high leakage currents, they are not suitable for applications above 150 ˚C. Higher band-gap materials, including III-Nitrides, are of interest in addressing this application gap at higher temperatures due to their excellent thermal stability and inert nature. To perform both steady state and dynamic pressure measurements, piezoresistive sensors utilizing the two-dimensional electron gas (2DEG) formed at the interface of AlGaN/GaN heterojunction, can be utilized. We will discuss potential applications of III-Nitride HEMTs as deflection sensors and high temperature pressure sensors.**

Keywords—III-Nitrides, pressure sensor, high electron mobility transistor, high temperature

I. INTRODUCTION

III-Nitride based microelectromechanical systems (MEMS), in spite of their strong promise, faced slow development for many years due to the growth of III-Nitride epilayers on substrates (SiC or sapphire) that are difficult to etch. With significant progress made in the growth of high quality III-Nitride layers on Si (111) substrates in recent years, the field of III-Nitride MEMS have started to expand rapidly. III-Nitride MEMS based RF filters,[1], pressure sensors, [2] acoustic sensors [3] and microcantilevers [4 - 7] have already been demonstrated. Our group has pioneered the development of highly sensitive resonant III-Nitride microcantilever based sensors that can detect pm level changes in oscillation amplitude transduced by the integrated AlGaN/GaN high electron mobility transistor (HEMT) at the microcantilever base.[7] The advantage of using a III-Nitride microcantilever is that due to the strong piezoresistive nature of III-nitrides, applied strain due to deflection of the microcantilever causes a change in 2-dimensional electron gas (2DEG) density (that carries the current) as well as effective mass, unlike Si where only the mobility is changed due to change in effective mass. The gate bias in the HFET allows the sensitivity to be tuned, and also helps to reduce the channel current and heating effects; hence the name piezotransistive microcantilevers.[7] AlGaN/GaN HFET deflection transducers, integrated at the base of GaN cantilevers, have resulted in very high gauge factor (GF) up to ~9000 under appropriate gate bias, [6], [7] which one of the highest reported so far for all transduction technologies, and is ~100 times more than Si piezoresistive cantilevers. This can be easily utilized in other MEMS devices such as pressure sensors.

High temperature operation of III-Nitride HEMT devices have been extensively studied to understand the device degradation mechanisms. At high temperatures, until at least 400 ℃, the 2DEG density and mobility, as well as the ohmic (source or drain) contacts do not degrade significantly even with continuous operation.[8] The gate schottky contact, however, degrades at higher temperatures, and significant research focus is being directed toward understanding and minimizing this gate contact degradation, and the consequent leakage current reduction. Nonetheless, high temperature operation of III-Nitride MEMS resonant sensors have been demonstrated with stable operation until 400 ℃.[8] Taken together, the above results clearly underlines the possibility of III-Nitride MEMS sensors to operate at higher temperature potentially utilizing AlGaN/GaN HEMTS to transduce deflection induced strain.

High temperature MEMS devices, such as pressure sensors have applications in aerospace, automotive, chemical processing, nuclear power and petroleum industries. While Si based piezoresistive pressure sensors are one of the most prevalent pressure sensors, due to degradation in their electrical properties related to the generation of thermal carriers and high leakage currents, they are not suitable for applications above 150 ˚C. Higher band-gap materials, including III-Nitrides, are of interest in addressing this application gap at higher temperatures due to their excellent thermal stability and inert nature. To perform both steady state and dynamic pressure measurements, piezoresistive sensors utilizing the two-dimensional electron gas (2DEG) formed at the interface of AlGaN/GaN heterojunction, can be utilized. The 2DEG will have both its density and mobility modulated as a function of strain, resulting in exceptional deflection sensitivity, much higher than Si piezoresistors, where only the carrier mobility is affected by strain. This can result in much higher deflection sensitivity (several 100 times higher) compared to the sensors utilizing Si based piezoresistive pressure sensors. In this paper, we will discuss the application of III-Nitride HEMTs in deflection sensing in MEMS devices an then discuss their applications in GaN membrane based pressure sensors for high temperature applications.

II. Fabrication and Characterizaiton of MEMS Devices

A. *Fabrication of Microcantilevrs with integrtaed HEMT deflection transducers*

High quality epitaxial wafer, which consists of 3 nm i-GaN cap later, 20 nm Al_xGaN (x = 0.25), 1 µm i-GaN, 0.3 µm buffer layer, and 675 µm Si layers, was purchased from NTT, Japan. The epitaxial layer structure of the wafer is shown in Figure 1, while the microcantilever fabrication process flow diagram is shown in Fig. 2. A brief description of the fabrication procedure is as follows: First, the HEMT area was defined for which a diced sample of the AlGaN/GaN wafer was deposited with SiO_2 as hard mask using Uniaxis plasma enhanced chemical vapor deposition (PECVD). Then patterning the AlGaN mesa with dimensions of 35 × 35 µm was done using SC1827 positive photoresist. The SiO_2 and AlGaN layers are etched using Plasma-Therm inductively coupled plasma (ICP) tool to define the HFET. After AlGaN etching, PECVD SiO_2 hard mask deposited again to define the microcantilever outline. ICP etching of SiO_2 and GaN was done after patterning of the microcantilever outline with NR-71 negative photoresist. Then the oxide hard mask was etched away using buffered oxide etchant. All metal contact depositions were done using soft mask patterning with NR-71 negative photoresist. Deposition of the metal stack of Ti (20 nm) /Al (100 nm) / Ti (45 nm) / Au (55 nm) were done using CHA e-beam evaporator. Then, the HFET ohmic contacts was formed with rapid thermal annealing process (SSI RTP). Schottky metal contacts of Ni (25 nm)/Au (375 nm) and deposited using the e-beam. After gate contact deposition, the probe metal stacks of Ti (20 nm)/Au (150 nm) were deposited using the e-beam evaporator as well. The back side of the cantilever chip is isolated with PECVD SiO_2 and then patterned using the negative photoresist. The cavity with suspended microcantilevers was outlined by etching the pattern area using SiO_2 layer. Finally, deep Si etching with Bosch process (STS ICP) was done from backside to release the microcantilevers. SEM images of the fabricated AlGaN/GaN HFET embedded GaN microcantilevers can be seen in Fig. 3. These microcantilevers are called "piezotransistive" as unlike their piezoresistive counterparts, their resistance and corresponding strain sensitivity can be controlled by the gate voltage.

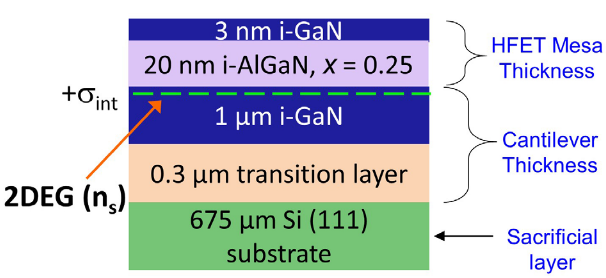

Figure 1. The epitaxial layer structure of the wafer that used to fabricate AlGaN/GaN HFET embedded piezotransistive GaN microcantilevers.

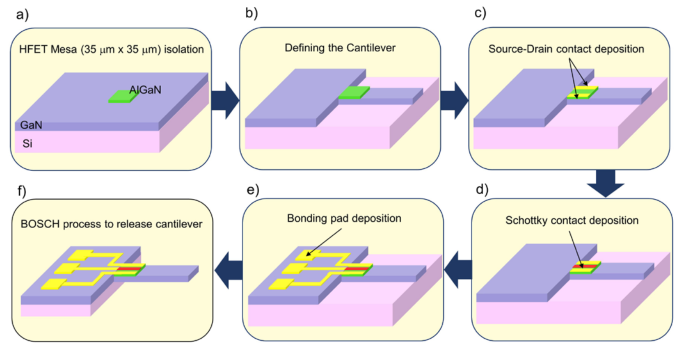

Figure 2. Fabrication process flow diagram for GaN microcantilevers. (a) Isolating the HFET location using ICP etching of AlGaN. (b) ICP etching of GaN to define the microcantilever area. (c) Ohmic contacts (drain and source) of Ti (20 nm) /Al (100 nm) / Ti (45 nm) / Au (55 nm) deposition using e-beam. (d) Deposition of Shottky-metal contacts of Ni (25 nm) / Au (375 nm) (e) Probe metal stack of Ti (20 nm) / Au (150 nm) deposited using the e-beam. (f) Deep Si etching with Bosch process to release the microcantilevers.

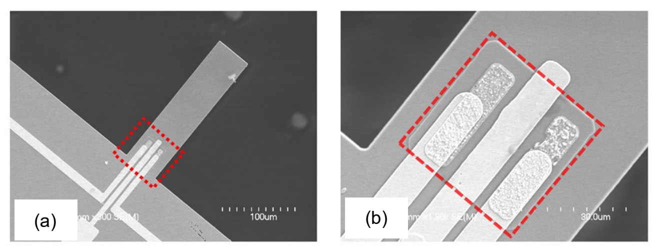

Figure 3. (a) SEM images of a 50 × 200 µm AlGaN/GaN HFET embedded GaN microcantilever. (b) Magnified image of the red dotted square in (a), showing close up view of the integrated HEMT.

III. Electrical and Mechanical Characterization

A. *Electrical Characterizaiton of the microcantilevers*

After fabrication, the electrical and mechanical properties of AlGaN/GaN HFET embedded piezotransistive GaN microcantilevers were characterized. The characterization procedure started with checking functionality of the HFETs. A dual channel source measure unit (SMU) (Keysight B2912A) was used to characterize I-V characteristics of the HFETs. In I_{DS}-V_{DS} measurements, the drain-source current, I_{DS}, was measured by varying the drain-source voltage, V_{DS}, at different constant gate voltages, V_{GS}. In I_{DS}-V_{GS} measurements, while supplying a constant V_{DS} (typically around 0.5 V), changes in I_{DS} due to sweeping the V_{GS} was measured. Typical I-V curves of AlGaN/GaN HFETs are shown in Fig. 4.

This work has been supported by the National Science Foundation through Grant # TI-2234512.

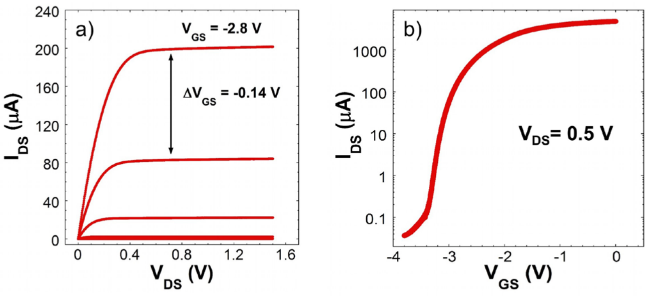

Figure 4. Typical I-V curves of AlGaN/GaN HFETs (a) I_{DS}-V_{DS} characteristics of AlGaN/GaN HFET embedded on GaN microcantilever with dimensions of 250 × 50 μm. The first I_{DS}-V_{DS} curve was taken at V_{GS} of -2.8 V. (b) I_{DS}-V_{GS} characteristics of the same HFET shown in (a) at V_{DS} voltage of 0.5 V.

B. Mechanical chracterization of the microcantilevers

Due to the strong piezoelectric properties of AlGaN/GaN heterostructure, applied strain can cause changes in both the 2DEG density and 2DEG mobility at the interface [21-25]. In Figure 3.7, the static bending experiment results of AlGaN/GaN HFET deflection transducers embedded on GaN microcantilever with dimensions of 250 × 100 μm are presented. A schematic of the experimental setup used for the AlGaN/GaN HFET embedded GaN microcantilever is presented in Fig. 5(a). A tungsten needle with a tip radius of 7 µm (72T-J3/70 Creative Devices Inc.) was attached to a computer-controlled nanopositioner (P-611.Z Physik Instrumente GmbH & Co.) for the static bending experiments. When the tip of the GaN microcantilever was bent 10 µm downward, the V_{DS} of the HFET under constant bias of I_{DS} = 200 µA and V_{GS} = 0 V was reduced by 0.15%. The current change was strongly correlated with the voltage bias. As shown in Fig. 5(b), increasing the deflection sensitivity of the AlGaN/GaN HFET by tuning the gate bias yielded 1% and 16% reductions in the V_{DS} at gate biases of V_{GS} = -2 V and V_{GS} = -2.5 V, respectively. As the cantilever bends downward, effective tensile stress increases the 2DEG density of AlGaN/GaN HFET, leading a reduction in the channel resistance of R_{DS}. At a constant I_{DS}, the HFET channel voltage of V_{DS} decreases by a percentage amount directly proportional to the R_{DS} reduction, as the cantilever undergoes a downward bending. Figure 5(c) displays the V_{DS} variation in Fig. 5(b) in terms of normalized R_{DS} changes ($\Delta R_{DS}/R_{DS}$) in the AlGaN/GaN HFET (red circles) at selected V_{GS}. As the 2DEG density reduced with more negative gate bias, the fractional change in the 2DEG became more, resulting higher sensitivity. [6]

IV. Electrical and Mechanical Characterization

A. Pressure sensor fabrication and characterization

The pressure transducers used in this study were also fabricated from wafers with similar layer structures as the microcantilevers following similar fabrication steps. At the beginning the top 100 nm of AlGaN/GaN layer was etched using BCl_3/Cl_2 plasma to define the mesa region at the periphery of the diaphragm, where the annular HEMT would be located to maximize strain. This was followed by deposition of Ti(20 nm)/Al(100 nm)/Ti(45 nm)/Au(55 nm) metal stack for ohmic contact formation. A rapid thermal annealing process was performed at 825 ºC for a minute, to form ohmic contacts for the source and drain regions for the HFET. After that, plasma enhanced chemical vapor deposition (PECVD) technique was used to deposit 100 nm thick SiO_2 to cover the open regions of the mesa, which served as the gate dielectric. This was followed by two consecutive stages of metallization, the first one had Ni(25nm)/Au(200 nm) stack as the gate metal contacts and the second one had Ti(20)/Au(225 nm) stack to from the probe contacts. Finally Bosch process was used from the bottom face of the sample to perform through wafer etching of silicon to release the diaphragm.

Figures 6(a) and (b) show the SEM images of a diaphragm from the topside and the backside of the sample. The sheet resistance of the AlGaN layer and the contact resistance of the ohmic metal pads were found out to be 316 Ω/sq and 19 Ω respectively, measured using transmission line measurement (TLM) technique.

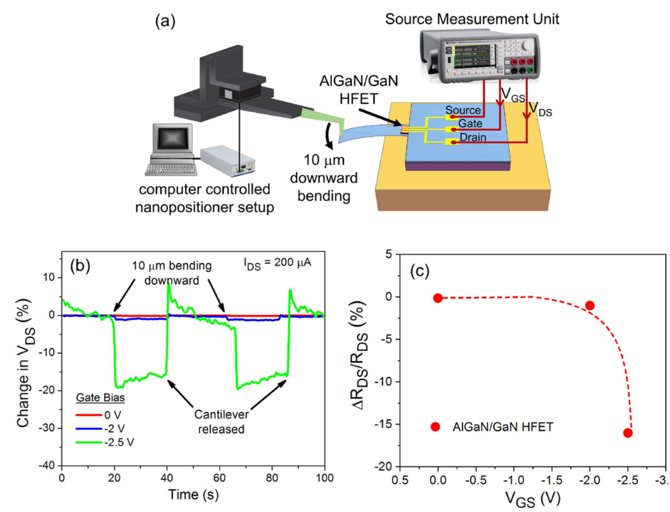

Figure 5 (a) Schematic of the experimental setup used to characterize the AlGaN/GaN HFET embedded GaN microcantilever through step bending of the cantilever apex. (b) 10 µm step bending results of AlGaN/GaN HFET embedded GaN microcantilevers at selected gate voltages. The HFET was biased at I_{DS} = 200 µA during downward bending experiments. (c) Calculated resistance changes of AlGaN/GaN HFET deflection transducers in response to 10 µm downward bending at selected gate biases.

For electrical and pressure transduction measurements, the HFET embedded diaphragms were glued to a printed circuit board (PCB) with a small pinhole in such a way that the pinhole is aligned with the diaphragm and the glue forms a vacuum seal. The contact pads were wire bonded and the PCB was mounted on a high pressure fixture shown in Fig. 1(d), where a gas line was installed beneath the diaphragm with high temperature O-rings for good vacuum sealing. A heater and a thermo-couple were also placed on top of the PCB, near the transducer chip, to carry out the experiments at higher temperatures.

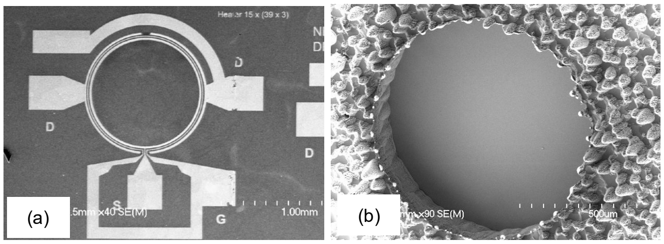

Figure 6. (a) SEM image from the top side showing the diaphragm (1 mm diameter) with integrated AlGaN/GaN HEMT deflection sensor at the periphery. (b) The back side SEM image of the diaphragm, where the pressure was applied for characterization.

B. Device characterizaiton and pressure sensing as a function of temperature

For electrical and pressure measurements as a function of temperature, the HFET integrated GaN membrane device was glued to a printed circuit board (PCB) with a small circular opening which aligned with the membrane, while a high temperature glue formed a vacuum seal.[9] The contact pads were wire bonded and the PCB was mounted on a test fixture as shown in Fig. 7, where a gas line was installed beneath the diaphragm with high temperature O-rings for good vacuum sealing. A heater and a thermo-couple were also placed on top of the PCB, near the transducer chip, to carry out the experiments at higher temperatures.

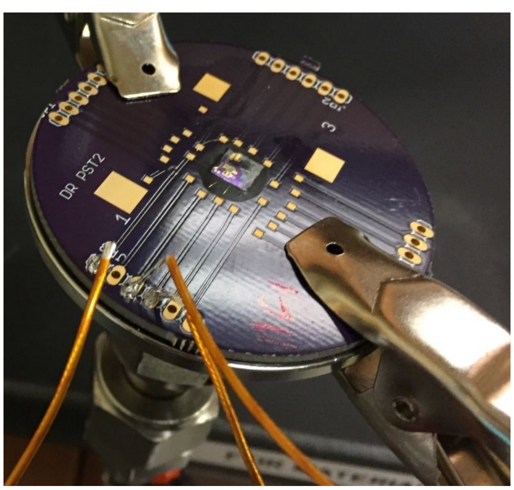

Figure 7. Experimental set-up for pressure sensing as a function of temperature.

Temperature dependent measurements of the drain current was carried out from room temperature to 200 °C and the results are shown in Fig. 8. We observe that the threshold and turn off voltages of the HFET were reduced with the increase of temperature. The threshold voltages of HFET at RT, 100ºC, 130ºC and 200ºC are approximately -7.5 V, -5.7 V, -4.9 V and -4 V respectively. This is in good agreement with the study of Alim et al on the variation of threshold with the temperature, where they also noticed that the positive shift in the Schottky barrier height along with trap-assisted phenomena shifted the threshold voltage towards positive values as temperature was increased.

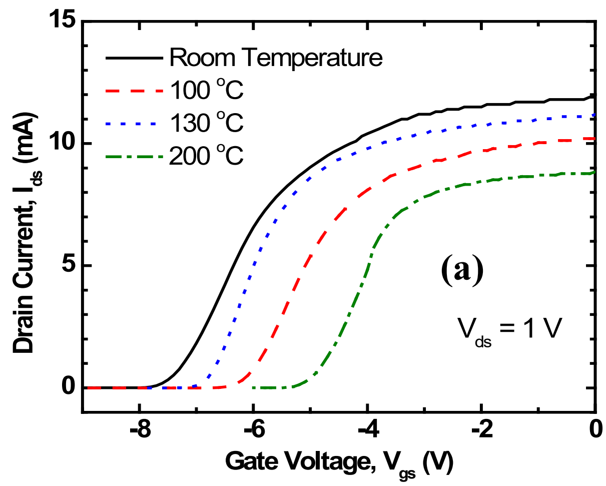

Figure 8. I_{ds}-V_{gs} characteristics of the HFET measured at different temperatures while the V_{ds} was maintained at a constant value of 1 V.

Figure 9(a) shows the variation of source-drain resistance (R_{ds}) as a periodic pressure of 20 kPa was applied to the GaN membrane at regular intervals, which resulted in an increase in R_{ds} as discussed earlier. The pressure was applied and released quickly using a valve to reduce mechanical transients in the measurements. For each measurement cycle, the differential pressure was kept at 20 kPa for ~20 s and then was reduced back to zero (atmospheric pressure). This was repeated for 4 cycles at various temperatures varying from room temperature to 200 °C. The results are compared in Fig. 9(b). For the measurements, the drain source voltage was kept constant at 1.5 V, while the gate voltage was tuned to achieve the highest sensitivity for each temperature. In Fig. 9(b), we see that the response magnitude and sensitivity increase from RT to 100 °C and then decrease slightly to 200 °C. The sensitivity of the pressure sensors varied from 0.022 kPa^{-1} with zero gate voltage to 0.5-0.76 kPa^{-1} in subthreshold region (gate biases -6 to -10 V) for different temperatures, with the maximum gauge factor (GF) being ~260. Clearly, even at higher temperatures the GF is much more than Si piezoresistive GF values which are typically less than 100 even at room temperature. With further optimization in the gate bias and the measurement set up, it is possible to further improve the device performance.

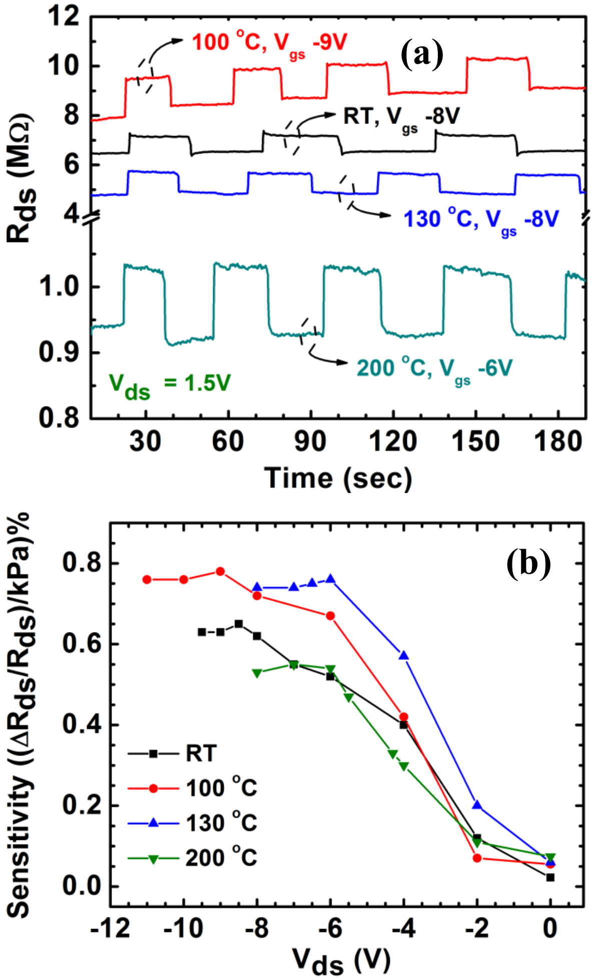

Figure 9. (a) The change in drain-source resistance R_{DS}, with periodically applied pressure of 20 kPa over multiple cycles is shown at temperatures varying from RT to 200 °C and constant drain voltage Vds of 1.5 V. (b) The variation of pressure sensor sensitivity with gate voltage bias, at different temperatures.

REFERENCES

[1] Yonghyun Shim, Jean-Pierre Raskin, César Roda Neve, Mina Rais-Zadeh, "RF MEMS passives on high-resistivity silicon substrates," IEEE Microwave and Wireless Components Letters 23, 632 (2013).

[2] J. Dzuba, G. Vanko, M. Držík, I. Rýger, V. Kutiš, J. Zehetner, and T. Lalinský. "AlGaN/GaN diaphragm-based pressure sensor with direct high performance piezoelectric transduction mechanism", Appl. Phys. Lett. 107, 122102 (2015).

[3] J. Segovia-Fernandez and S. Sonmezoglu and S. T. Block and Y. Kusano and J. M. Tsai and R. Amirtharajah and D. A. Horsley, "Monolithic piezoelectric Aluminum Nitride MEMS-CMOS microphone," 2017 19th International Conference on Solid-State Sensors, Actuators and Microsystems (TRANSDUCERS), Kaohsiung, 2017, pp. 414-417.

[4] Muhammad Qazi, Nicholas DeRoller, and Goutam Koley, "Piezoresistive microcantilever with embedded AlGaN/GaN HFET for sensing applications," Applied Physics Letters 99, 193508 (2011).

[5] Abdul Talukdar, Muhammad Qazi and Goutam Koley, "High frequency dynamic bending response of piezoresistive GaN microcantilevers," Applied Physics Letters 101, 252102 (2012).

[6] Abdul Talukdar and Goutam Koley, "Impact of Biasing Conditions on Displacement Transduction by III-Nitride Microcantilevers," Electron Device Letters 35, 1299 (2014).

[7] Abdul Talukdar, M. Faheem Khan, Dongkyu Lee, Seonghwan Kim, Thomas Thundat and Goutam Koley, "Femtoscale displacement transduction using piezotransistive GaN microcantilever," Nature Communications 6, 7885 (2015).

[8] S. Kargarrazi, A. S. Yalamarthy, P. F. Satterthwaite, S. W. Blankenberg, C. Chapin and D. G. Senesky, "Stable Operation of AlGaN/GaN HEMTs for 25 h at 400°C in air," in IEEE Journal of the Electron Devices Society, vol. 7, pp. 931-935, 2019.

[9] Durga Rao Gajula, Ifat Jahangir, and Goutam Koley, "High temperature AlGaN/GaN membrane based pressure sensors," Micromachines 9, 207 (2018).